Development of a subgrid scale parameterisation of mountain glaciers for use in regional climate modelling

Sven Kotlarski, Daniela Jacob
Max Planck Institute for Meteorology, Hamburg, kotlarski@dkrz.de

Introduction

The proper description of cryospheric processes is essential for simulating the complete terrestrial water cycle in climate models. Besides the large polar ice sheets, this is especially true for alpine river catchments where the regional climate as well as seasonal runoff patterns are strongly influenced by the presence of glaciers (Singh and Singh, 2001; Jansson et al, 2003). In order to simulate the two-way interaction between glaciers and climate, existing models for both components have to be merged. So far, the terrestrial cryosphere is represented in an extremely simplified way in most state-of-the-art global and regional climate models (GCM and RCM). Static glacier maps are used indicating whether a specific climate model grid box is covered by land ice or not. These maps remain constant throughout the model integration and the glacierised surface area is kept unchanged even in case of pronounced snow accumulation or melting of snow and ice. Furthermore, runoff generation is usually neglected over ice covered areas.

This simple approach is suitable for short model integrations and for large ice sheets with a slow response to climatic forcing. For longer simulations and especially for assessing regional climate change effects and its impacts on runoff regimes in alpine regions, a more detailed description of processes related to mountain glaciers is required. Therefore, a subgrid scale parameterisation of mountain glaciers is being developed and implemented into the regional climate model REMO (Jacob, 2001). The new scheme expands and partly replaces the static glacier mask used so far and includes the most important processes governing the extent of mountain glaciers and their potential influence on regional climate and runoff conditions.

The New Mountain Glacier Scheme

In order to account for glacierised surfaces on a subgrid level, land ice is introduced as a fourth possible surface fraction of a REMO grid box in addition to ice-free land, water and sea ice. The sum of all four sub areas equals the total grid box area. Turbulent surface fluxes are derived separately for each fraction by applying a bulk transfer relation with transfer coefficients derived form Monin-Obukhov similarity theory. Fluxes are subsequently averaged within the lowest atmospheric level using the corresponding surface fractions as weights (*tile approach*).

The total land ice mass of a specific grid cell is represented by one single glacier covering a certain fraction of the total grid box land area (Fig. 1). The glacial body consists of two layers: a surface layer of 10 cm thickness and a bottom layer representing the main ice mass. Both the glacierised and the non-glacierised surface fraction can be covered by a snow layer and share a common soil consisting of five temperature layers. The surface albedo of glacier ice is a linear function of ice temperature of the upper layer and varies between 0.4 ($T_{ice} \leq -10°C$) and 0.3 ($T_{ice} = 0°C$). Meltwater of the upper ice layer directly contributes to surface runoff while meltwater originating from the bottom layer is an additional water input for the soil surface and is subsequently divided into surface runoff and infiltration. So far, no additional storage or refreezing of meltwater within the ice is implemented.

Snow on the glacierised and non-glacierised surface fractions can be transformed into glacier ice once a continous snow cover of 730 days is reached. In order to account for the fact that within a REMO grid box glaciers are assumed to be located at higher altitudes (= lower mean air temperature) rather than in lowland areas, a part of the total grid box snow fall rate is redistributed from the non-glacierised surface fraction to the glacier. Ice flow processes within a grid box are not explicitly accounted for. Instead, the size of the glacierised area is controlled by a simple volume area relation which is based on a power law (Bahr et al., 1997):

$$V = c * A^{\gamma} \qquad (1)$$

with glacier volume V [m^3] and glacier area A [m^2]. The constant c and the scaling parameter γ are taken from Chen and Ohmura (1990) who tuned c to 0.206 and γ to 1.357 based on data from 63 alpine glaciers. Ice flow between adjacent grid boxes is totally neglected in the presented parameterisation. Glaciers in neighbouring grid cells do not interact directly which restricts the usage of the new scheme to mountain glaciers and small ice caps where large scale ice flow processes can be neglected.

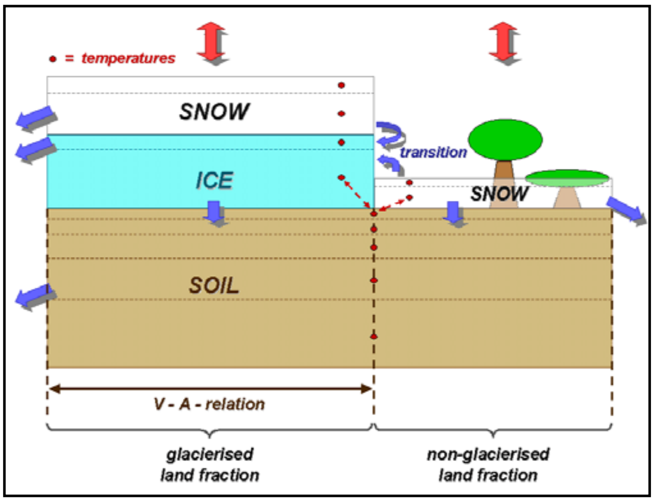

Fig. 1: Schematic overview of the new mountain glacier scheme.

Experimental Setup

A first 10-year test simulation for the period 1979-1988 has been performed using REMO version 5.3 with the fully coupled mountain glacier scheme. The regional model domain covers the European Alps with a horizontal resolution of $^1/_6°$ (approx. 18 x 18 km grid box size) and 20 vertical levels. Lateral forcing as well as atmospheric initial conditions are provided by a REMO ½° simulation which in turn is driven by ERA15 reanalysis (double nesting technique). Initial ice temperatures were set to 0°C for the entire domain. Glacierised area and mean ice depth for the single REMO boxes were initialised using data of the World Glacier Inventory (NSIDC, 1999). The resulting glacierised surface fraction at initialisation is lower than 10% for most grid cells

However, maximum values of up to 50% are reached in the Swiss Alps, where maximum mean ice depth lies between 90 and 100 m icepack (not shown).

Results

After 10 years of model simulation, almost all grid cells show a decrease of glacierised area (Fig. 2). The relative decrease is largest in grid cells with a low grade of glaciation in 1979 and reaches up to 100% (total disappearance of glaciers). The larger the ice covered area at initialisation, the smaller the relative loss of area. This is at least in parts a direct effect of the larger volume-to-surface ratio of highly glacierised boxes due to the positive relationship between glacier area and ice depth derived from eq. (1). Three REMO boxes, however, show a slight increase of glacierisation (up to 8 %). The overall decrease of ice covered area in the model domain between January 1979 and December 1988 is –45.5%, which is too high compared to observed area changes. PAUL et al. (2004) estimate a relative decrease of glacier area in the Alps of only 22% for the period 1973-1999, including the stabilisation period until 1985 and a strong retreat thereafter.

In order to verify ongoing processes and to find possible reasons for too high melt rates, two REMO grid cells have been analysed in more detail. These boxes are located in the western part of the Alps and have an initial degree of glaciation of 22.5% and 33.6% respectively (Fig. 3 a). After 10 years of continuous simulation, the glacierised area fraction of box A decreased down to 10.9% (-51.6%) while Box B shows a slight increase of ice cover (+0.6%). The pronounced melting of snow and ice in Box A leads to mean monthly runoff peaks of > 40 mm/day in summertime (Fig. 3 b). The presence of snow on top of the ice surface throughout the whole year in box B (Fig. 3 c) also prevents the ice from being melted which at least partially explains the stable ice volume in this grid cell. A further reason for the pronounced melt rates in box A is the higher amount of net surface radiation in summertime with energy input exceeding 100 W/m² (Fig. 3 d). This is partly due to the disappearance of snow in summer which exposes the darker ice surface and increases absorption of solar radiation via decrease of surface albedo. The surface sensible heat fluxes are positive throughout most parts of the year (energy flux from air to surface) but only reach maximum values of about 45 W/m² (Fig. 3 e) which is small compared to radiation fluxes. We therefore assume that the reason for too high melt rates throughout the model domain lies in processes connected to radiation and in the internal distribution of temperature within the glacier rather than in too high air temperatures (caused for example by the neglection of subgrid scale orography). However, both possibilities will be investigated in more detail in the near future. A special regard will be paid to comparison of simulated and observed air temperatures above glacierised surfaces.

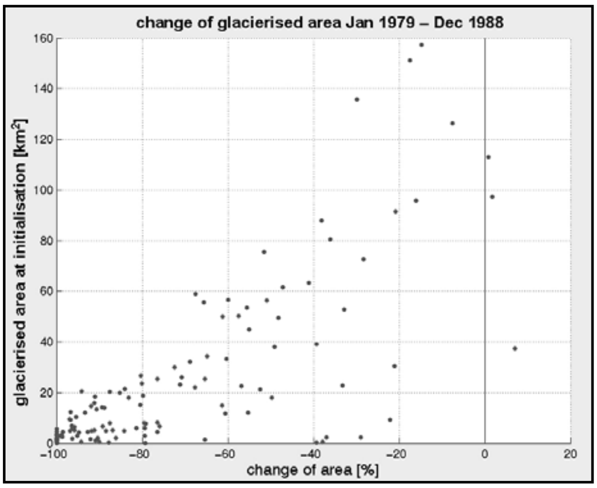

Fig. 2: Change of glacierised area [%] after 10 year model simulation (each dot represents a single REMO grid box).

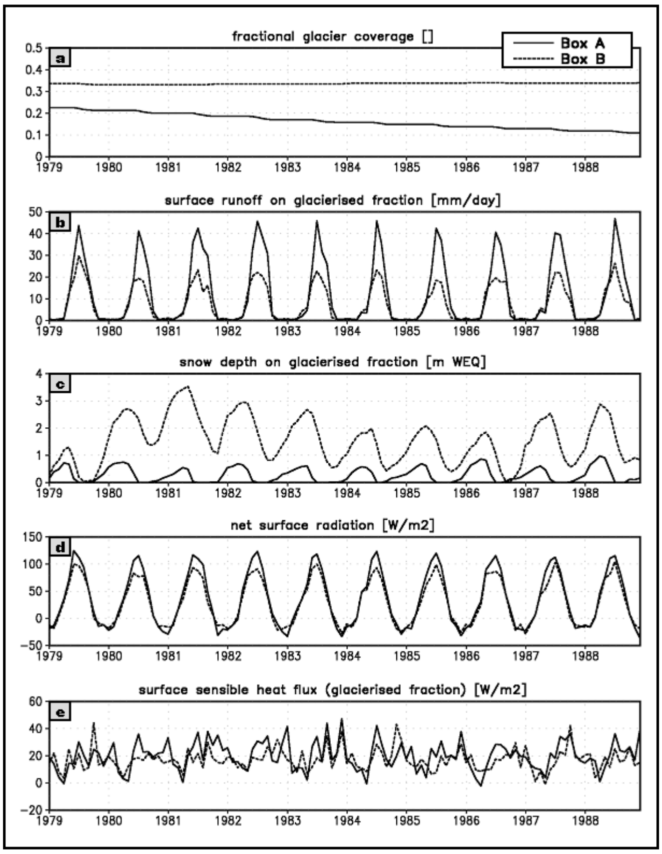

Fig. 3: Evolution of different surface parameters for grid boxes A and B throughout the 10-year simulation period (monthly mean values).

References

BAHR, D., MEIER, M., PECKHAM, S. (1997): The physical basis of glacier volume-area scaling. *J. Geophys. Res.* 102: 20 355 – 20 362.

CHEN, J. and OHMURA, A. (1990): Estimation of Alpine glacier water resources and their changes since 1870s. In: Hydrology in Mountainous Regions. I – Hydrological Measurements; the Water cycle. IAHS publ. 193: 127-135.

JACOB, D. (2001) : A note to the simulation of the annual and inter-annual variability of the water budget over the Baltic Sea drainage basin. *Meteorol. Atmos. Phys.* 77, 61-73.

JANSSON , P., HOCH, R., SCHNEIDER, T. (2003) : The concept of glacier storage : a review. *J. Hydrol.* 282, 116-129.

NSIDC (1999). World Glacier Inventory. World Glacier Monitoring Service and National Snow and Ice Data Center/World Data Center for Glaciology. Boulder, CO. Digital media: http://nsidc.org/data/glacier_inventory

PAUL, F., KÄÄB, A., MAISCH, M., KELLENBERGER, T., HAEBERLI, W. (2004): Rapid disintegration of Alpine glaciers observed with satellite data. *Geophys. Res. Lett.* 31, No. 21, L21402.

SINGH, P. and SINGH, V. (2001): Snow and glacier hydrology. Kluwer Academic Publishers, 742 pp.